

QUT Digital Repository:
<http://eprints.qut.edu.au/>



Nami, Alireza and Zare, Firuz and Ghosh, Arindam and Blaabjerg, Frede (2009)
Cross voltage control with inner hysteresis current control for multi-output boost converter. In: Proceedings of European Conference on Power Electronics and Applications (EPE), 8-10 September 2009, Palau de Congressos de Barcelona, Barcelona.

© Copyright 2009 IEEE

Cross Voltage Control with Inner Hysteresis Current Control for Multi-output Boost Converter

Alireza Nami, Firuz Zare, Arindam Ghosh
 School of Electrical Engineering
 Queensland University of Technology
 GPO Box 2434, Brisbane,
 QLD, 4001, Australia
 E-mail: namia@qut.edu.au

Frede Blaabjerg,
 Aalborg University, Aalborg, Denmark
 Institute of Energy Technology, 9220
 Alborg East, Denmark
fbl@iet.aau.dk

Acknowledgment

The authors thank the Australian Research Council (ARC) for the financial support for this project through the ARC Discovery Grant DP0774497.

Keywords

Multi-output boost converter, hysteresis current control, voltage control

Abstract

Multi-output boost (MOB) converter is a novel DC-DC converter unlike the regular boost converter, has the ability to share its total output voltage and to have different series output voltage from a given duty cycle for low and high power applications. In this paper, discrete voltage control with inner hysteresis current control loop has been proposed to keep the simplicity of the control law for the double-output MOB converter, which can be implemented by a combination of analogue and logical ICs or simple microcontroller to constrain the output voltages of MOB converter at their reference voltages against variation in load or input voltage. The salient features of the proposed control strategy are simplicity of implementation and ease to extend to multiple outputs in the MOB converter. Simulation and experimental results are presented to show the validity of control strategy.

Introduction

The multi-output DC-DC converter is an efficient and economical device which uses instead of several separate single output converters to build multi-output power supply [1]. The MOB converter with N series output voltages is shown in Fig. 1.

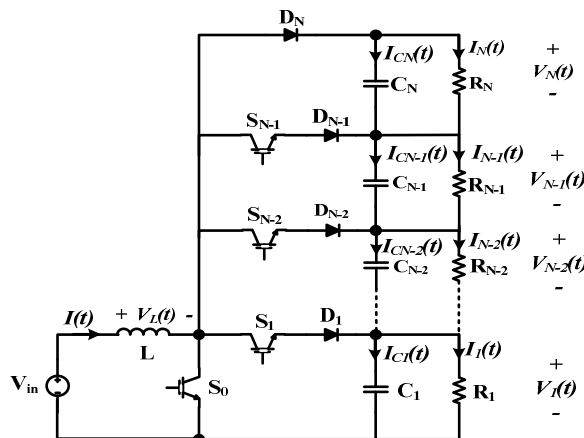


Fig.1: Configuration of new DC-DC MOB converter with N-output

The steady state and dynamic analysis of this converter for double-output are addressed in [2]. This converter has been developed based on a boost converter structure with extra sharing switches which lead to sharing output voltage. This type of converter can benefit systems using multiple series power regulator such as transformerless grid connected renewable energy systems based on diode-clamped converters where capacitor voltage balancing is a crucial problem. As the main structure of MOB is similar to boost converter topology, it suffers from Right half-plan zero (RHPZ) and its relationship to the amount of load regarding its input to output transfer function continuous-conduction mode (CCM)

which leads to instability and some limitations. A common solution to reduce the effect of this problem in converters with RHPZ is to employ the current-mode control [3,4]. Several current-mode control strategies have been conducted to increase the dynamic response and application in a wide range of operations of RHPZ converter systems [4-7]. Digital current controller implemented in DC-DC converters in [8,9] to have a simple control realization which combine the advantages of digital and current mode. In this paper, a current control strategy combined with voltage control has been utilized to keep the simplicity of the system as it can be extended from a double-output converter to a multi-output converter without a significant change in the control circuit. This control strategy may be implemented with a combination of analogue and logical ICs, or a simple microcontroller to keep the output voltages of the MOB converter at desired voltages against variation in load or input voltage. Simulation and experimental results have been presented to show the validity of the control strategy and operation of proposed configuration.

Configuration and limitation

A circuit diagram of the double-output boost converter is shown in Fig.2 (a). This circuit consists of a boost switch S_0 , sharing switches S_1 , two diodes (D_1 to D_2), an inductor L , and two capacitors (C_1 to C_2) with different loads (R_1 to R_2).

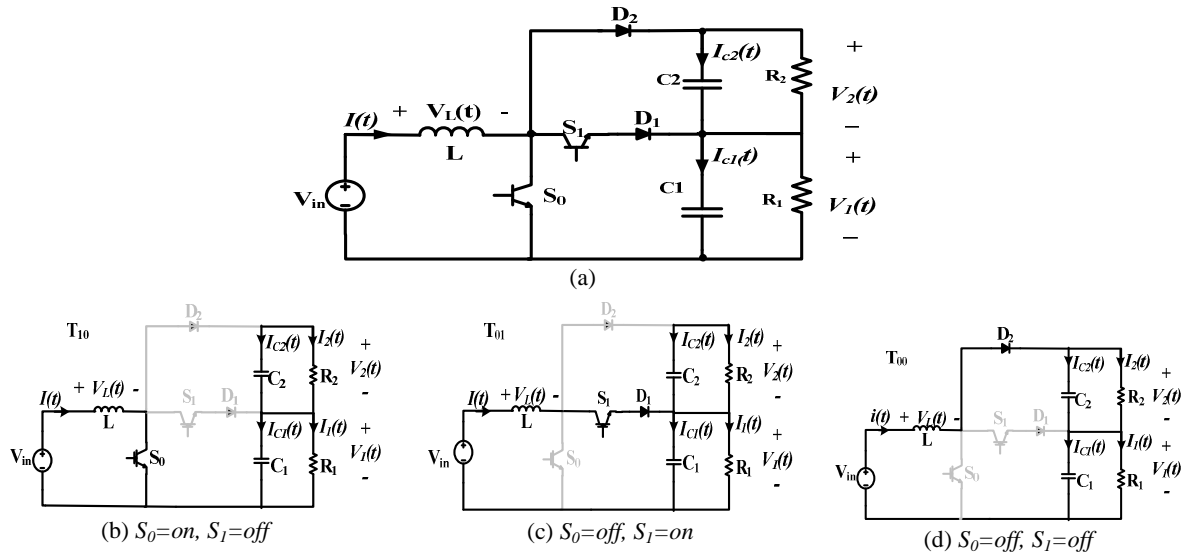


Fig.2: Configuration of double-output boost converter (a) schematic; (b)-(d) equivalent circuit in different switching intervals for double-output

In the subinterval zero, S_0 is turned “on” and the inductor can be charged by the current flowing through it. In the next two subintervals, S_0 remains “off” and the S_1 is switched to charge capacitors at the desired value. When S_1 is “off”, the diode (D_2) directs the inductor current to charge all C_1 and C_2 to generate V_1 to V_2 , respectively. D_1 is used to block the negative voltage and provide two quadrant operation of S_1 . In a double-output converter, there are three possible switching states as S_1 can not be turned “on” while S_0 is “on”. The operation of the circuit in three different switching states has been summarised in Table I. The equivalent circuits of all switching states have been demonstrated in Fig.2 (b) to 2(d).

Table I: Switching states of double-output boost convert

Switching states	S_0	S_1	C_1	C_2
10	on	off	Discharge	Discharge
00	off	off	Charge	Charge
01	off	on	Charge	Discharge

To analyse the steady state performance of the MOB converter, the time intervals for each switching are considered as T_{10} , T_{00} , and T_{01} . Then, switching period can be expressed as follows:

$$T_{10} + T_{00} + T_{01} = T \quad (1)$$

the operation of the MOB converter in three different switching states in continuous conduction mode (CCM) steady state equation as follows [1];

$$\begin{cases} V_1 = \frac{n(D'_0)V_{in}}{n(D'_0)^2 + (D_0 + D_1)'^2} \\ V_2 = \frac{(D_0 + D_1)'V_{in}}{n(D'_0)^2 + (D_0 + D_1)'^2} \\ I = \frac{V_{in}}{R_1(D'_0)^2 + R_2(D_0 + D_1)'^2} \end{cases} \quad (2)$$

where, $(D_0 + D_1)' = \frac{(T_{00})}{T}$ and $D'_0 = \frac{(T_{00} + T_{01})}{T}$. Since the output voltage in Eq.2 is related to the load ratio, Table II shows some limitations to achieve diverse voltages that should be considered due to the fundamental nature of the circuit. While $\frac{(D_0 + D_1)'}{D'_0} < 1$, restriction happens when $V_1 < V_2$ where n must be less than one.

Table II: Nature limitation of load ratio in different output voltage

$V_1 = V_2$	$n = \frac{(D_0 + D_1)'}{D'_0}$
$V_1 > V_2$	$n > \frac{(D_0 + D_1)'}{D'_0}$
$V_1 < V_2$	$n < \frac{(D_0 + D_1)'}{D'_0}$

Based on averaging method in each switching a dynamic model and transfer function for the proposed circuit are:

$$s \begin{bmatrix} L & 0 & 0 \\ 0 & C_1 & 0 \\ 0 & 0 & C_2 \end{bmatrix} \begin{bmatrix} i \\ v_1 \\ v_2 \end{bmatrix} = \begin{bmatrix} 0 & -(D'_0) & -(D_0 + D_1)' \\ (D'_0) & -\frac{1}{R_1} & 0 \\ (D_0 + D_1)' & 0 & -\frac{1}{R_2} \end{bmatrix} \begin{bmatrix} i \\ v_1 \\ v_2 \end{bmatrix} + \begin{bmatrix} 1 \\ 0 \\ 0 \end{bmatrix} V_{in} \quad (3)$$

According to Eq.3, changing $(D_0 + D_1)'$ and D'_0 with different ratio in a close loop control system can keep the output voltages constant while the inductor current value has been modified. Developing this concept will lead to a current control strategy in cooperation with voltage control to achieve desired output voltage sluggishness of dynamic response. Regarding steady state statements and dynamic model, proposed MOB converter acts as a boost converter topology with series multi-output voltages.

Control strategy and switching scheme

In this paper simplicity of control strategy and cost effectiveness of implementation have been considered as the structure blocks applied in this control strategy may be realized by logical elements or simple micro controller. In order to have the potential of combining advantages of logic control and current mode control in a relatively simple controller realisation for the MOB converter, a cross voltage control (V_T) with an internal hysteresis current control loop has been performed combined with a mid point voltage (V_I) control. Fig.3 illustrates the block diagram of the control method for a double-output boost converter. As shown, the solid loop is a cross voltage control with a hysteresis current control loop for the inductor current, in which the cross output of the MOB converter is controlled by switching the boost switch (S_0). The dashed loop is a mid point voltage control where a sharing switch (S_I) is forced to balance the capacitors' voltage.

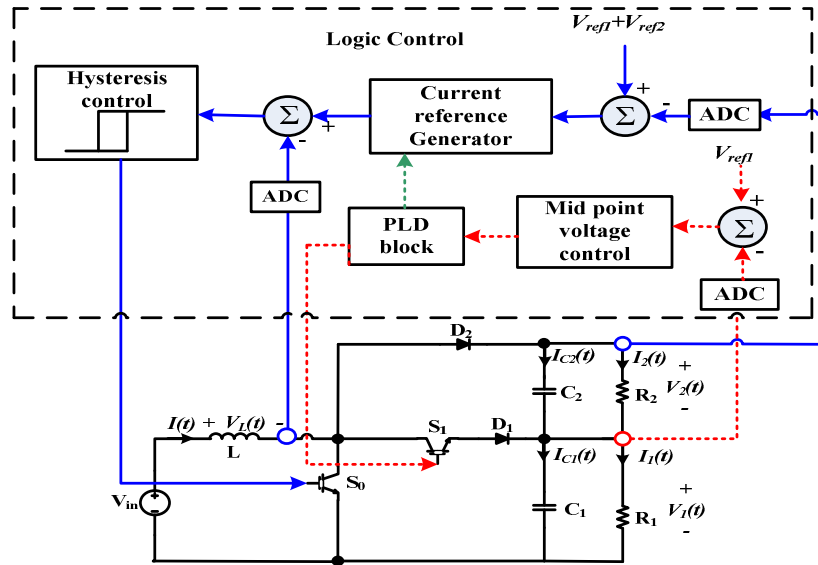


Fig.3: Block diagram of the proposed control system

Total voltage control with hysteresis current control loop

This control loop consists of two cascaded control loops. The outer loop is a voltage control mode through which the reference current is modified according to voltage error to force this error to zero. The inner loop is the hysteresis current control which is the main loop that runs to forcibly constrain the inductor current between the hysteresis bands around the defined reference current.

Current reference generator block

Since the both output voltage and inductor current are controlled by the boost switch (S_0), so that overshoot (undershoot) occurs when the load is decreased (increased) due to inappropriate inductor current. To find the correct current reference against any disturbance in load or input voltage, the reference current generator applies based on the level of total output voltage error. The reference current is modified discontinuously in discrete time to predict the desired inductor reference current to force the voltage error to zero. The signal to update the reference current is generated from the PLD block. The reference current will be decreased (increased) whenever the error is more (less) than a dead band. Subsection "1" in Fig.4 shows the flowchart of this control section. There is a gain (G) for closed loop control to change the step change of the reference current. Therefore, dynamic response is a function of current step change which is defined by three following criteria:

- Output voltage error,
- Gain of the close loop system
- Discrete time for current modification

As the voltage error depends on disturbance in load or input voltage, close loop gain and discrete time are the control parameters. The gain should be increased when the error is high and decreased when the error is low to improve the dynamic response. On the other hand, current step change to improve dynamic response can be applied based on discrete time instead of changing close loop gain. Thus, discrete time should be small (big) when the voltage error is high (low). Therefore, current step change can be adapted according to the voltage error to achieve a good dynamic response. Controlling the dynamic response by discrete time is chosen in this paper as it is easy to implement by logical devices. To do so, discrete time can be defined based on number of distinct hysteresis pulses generates from hysteresis control block. .Current generator block can be implemented by a sample and hold IC which can keep the current reference as an analogue signal and modify it based on the error signal. Also, a microcontroller can generate a reference current according to the error.

Current hysteresis block

This block changes its output signal based on comparing the actual inductor current and its reference to track the reference current. Therefore, once the inductor current error hits the upper (lower) band, the output signals change to zero (one). In this manner, the inductor current is controlled in defined

hysteresis band. The output of the hysteresis block applies to a Programmable Logic Device (PLD) block and the boost switch S_0 . Since the S_0 is controlled by the hysteresis current control, the control law is defined as Eq.4.

$$\begin{cases} \text{if} & I \geq I_{ref} + B & \text{then} & S_0 = 0 \\ \text{if} & I \leq I_{ref} - B & \text{then} & S_0 = 1 \end{cases} \quad (4)$$

where, I , I_{ref} , B are the inductor actual current, inductor reference current, and hysteresis band height respectively. The control scheme of the hysteresis current control is depicted in subsection “2” in Fig.4. This block can be implemented by a logic device or a simple program in a microcontroller.

Mid point voltage control

Due to the nature of the proposed converter in Table I, there is no chance to turn S_0 and S_1 “on” simultaneously. To balance the mid point of capacitors, only two switching states are utilisable (00 and 01). Although there is no chance to charge the C_2 regardless of C_1 , the reference current generator can modify the total voltage ($V_T=V_1+V_2$) in this case. In the dead band voltage control block, the amount of mid point voltage (V_j) error is compared with the defined voltage dead band (assumed 1% of reference), if the voltage is higher than the upper (lower) dead band output signal of block changes to one (zero). The output signal applies to the PLD block. The control scheme flowchart of the mid point voltage control is shown in subsection “3” in Fig.4. Subsection “3” is the only control section that has to be added to force the sharing switches in a converter with more than two output voltage by measuring the related mid point voltages.

Programmable logic device (PLD)

This block involves two tasks. The first is designed to count the hysteresis pulses and enable signal for current reference generator block after a defined hysteresis pulses frequently. By doing so, the current reference does not change faster than the inductor current dynamics. Furthermore, the inductor reference current can change within a different number of hysteresis pulses to control the dynamic response.

The second task is to apply a proper switching state for S_1 to balance the mid point voltage. To do so, the best switching state is chosen from Table III to make an optimum balance between the actual output voltages and their references, during the discharging period of the inductor ($S_0=off$) in each switching cycle. Therefore, the duty cycle of S_1 (D_1) is defined to balance the mid point voltage. By receiving the digital signals from hysteresis and mid point voltage control block, proper signals for the current generator block and S_1 are generated by the PLD block, so that it can be implemented with a logic device or programmed in a microcontroller.

Table III: Switching states based on V_j position

Position of V_j	Switching state of S_0	Switching state of S_1
V_j is below the reference voltage	$S_0=0$	$S_1=on$
V_j is above the reference voltage	$S_0=0$	$S_1=off$

Switching pattern and flowchart of control strategy

The entire flowchart of the proposed control strategy has been depicted in Fig.4. As illustrated, except for changing the inductor reference current that can be implemented with an analogue sample and hold IC, the other parts of the control are based on logic signals. Also, control circuit can easily be applied for multiple outputs by measuring the mid point voltages and controlling the relevant sharing switch of that point with the mid point voltage control. The switching pattern of S_0 and S_1 based on hysteresis block pulses and mid point voltage control has been demonstrated in Fig.5. In the hysteresis current control, the hysteresis band of the current regulator is adjusted to control the switching frequency. By assuming the hysteresis band height as $2B$, the switching frequency can be calculated as follows:

$$2B = \frac{D_0 T V_{in}}{L} \Rightarrow f_{sw} = \frac{V_{in} D_0}{2LB} \quad (5)$$

In Eq.5, switching frequency is defined based on hysteresis band height, rate of inductor, input voltage, and duty cycle. Therefore, by considering the constant hysteresis band and circuit parameter, the switching frequency is constant whenever the ratio of loads ($n = \frac{R_1}{R_2}$) is constant.

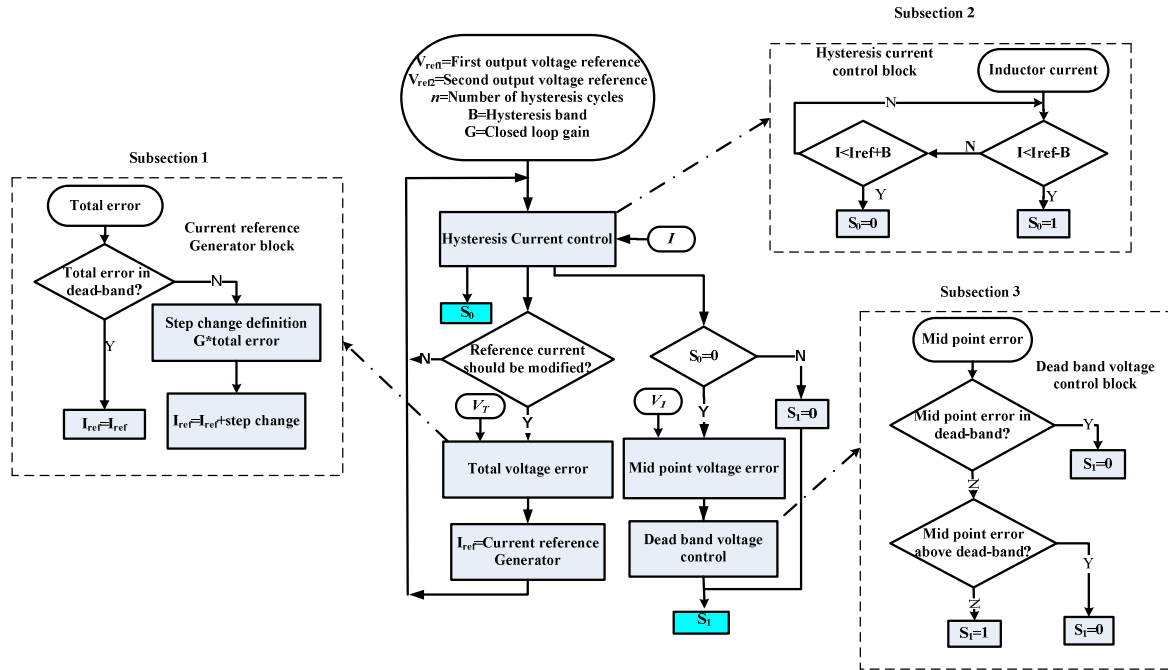


Fig.4: Flowchart of Control strategy for double-output MOB converter

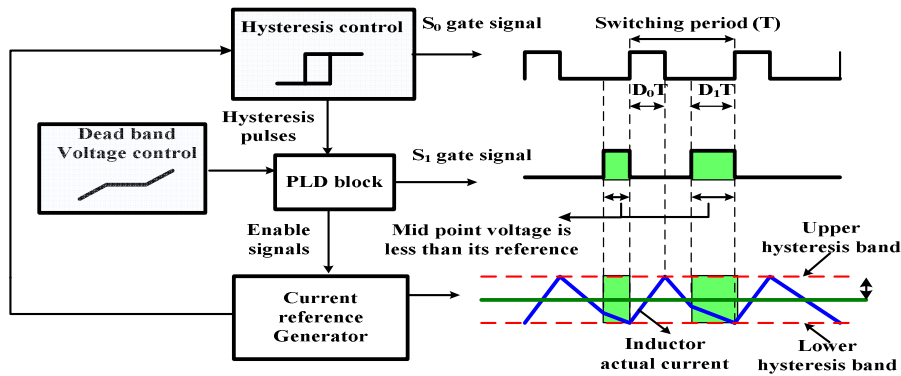


Fig.5: Switching pattern of S_0 and S_1 based on control strategy

Simulation results

To show the performance of the proposed converter under the presented control strategy, simulations in different conditions with load variation have been performed. In all simulations $L=1mH$, $C_1=C_2=0.1mF$, $V_{in}=10V$, and the total output voltage (V_T) has been boosted to 30V. To show the ability of the system to control the mid point voltage (V_I) to the different value, it has been set for 20V which is twice the input voltage. As discussed, the time for modification of current reference and closed loop gain are the parameters in the control strategy which can affect the dynamic response. A controller function to generate a proper reference current against a load variation is simulated in Fig. 6(a), when the voltage is dropped due to an increment in load current. As it is exposed, the inductor reference current modification is proportional to the voltage error and it occurs after defined enable time. To show the dynamic response behaviour associated with distinct time for current modification, three different modification times, one, five, and ten hysteresis cycles have been examined with the same load disturbance and constant closed loop gain ($G=0.001$). Fig.6 (b) to 6 (d) illustrate the dynamic performance of the control scheme against variation in load. As shown, there is instability in control system when the current modification occurs too fast in each hysteresis cycle (Fig.6 (b)). When the current changes too fast, it can increase the dynamic response but due to the fast change, the inductor current reaches to zero and control became instable. On the other hand, when discrete time is five or ten hysteresis cycles the reference current has been updated based on voltage error to achieve the desired output voltages in Fig.6 (c) and (d). Increasing the enable time helps to increase the stability of

the control strategy, however, it reduces the response of the system. According to simulation results for step time change with five and ten hysteresis cycles, modification with five hysteresis cycle shows a faster response and lower overshoot and undershoot in comparison with ten hysteresis cycles modification.

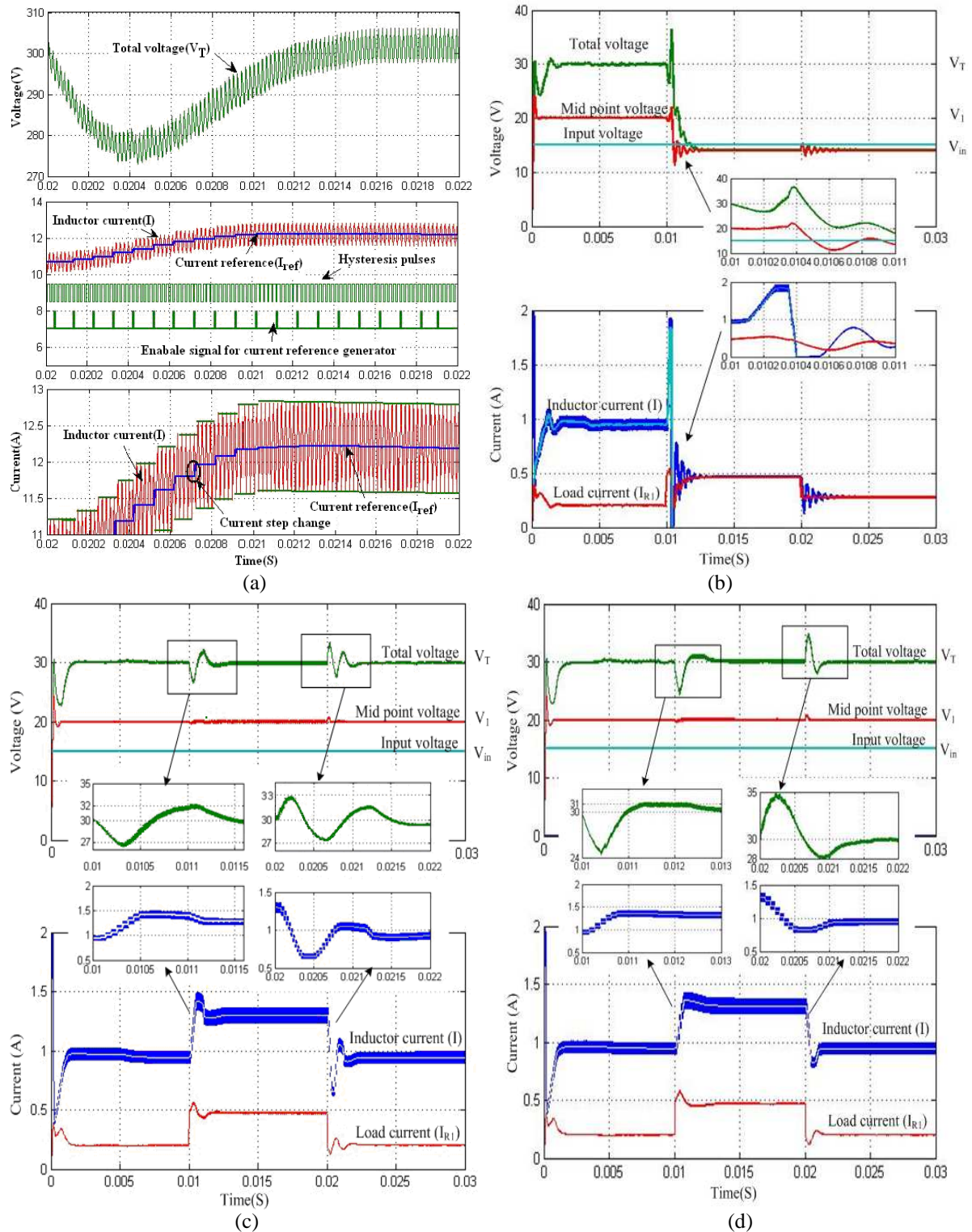


Fig.6: Dynamic operation of controller during load transient (a) generate desired reference current (enable signals comes after five hysteresis cycle). (b) current modification in each hysteresis cycles. (c) current modification in five hysteresis cycles. (d) current modification in ten hysteresis cycles. R_l is changed from 50Ω to 25Ω and back at $0.01s$ and $0.02s$

Hardware results

To verify the proposed MOB converter with the control strategy, a prototype of a double-output converter has been developed and controlled. The instantaneous values of the inductor current and output voltages are used to compare the threshold values given by the hysteresis current control and the dead band voltage control respectively. In the laboratory prototype, two SK50 Gal 065 switches, which is a compact design of the IGBT and diode module suitable for the boost converter, are used as the main switching devices; S_0 , S_1 , and D_2 . Also, an ultrafast diode ($MUR820G$) has been used in series with S_1 . In the controller part, the $NEC V850E/IG3$ microcontroller has been utilised to implement the control strategy. Skyper 32-pro is used as a gate driver, which can drive two switches independently and is compatible with the utilised IGBT module. Also, the load disturbances are applied using toggle switches. As the power supply used in the laboratory has current-limiting protection, the test has been conducted at low voltage. In all tests, the mid point voltage (V_I) and total output (V_T), are assumed to be kept at $20V$ and $30V$ respectively, while $V_{IN}=15V$. The steady-state response under the proposed control scheme is shown in Fig.7. The switching pulses (control signal) and the inductor-current waveforms are shown in Fig.7 (a) for the CCM operation of the converter with load resistances of $R_1=R_2=50 \Omega$. From the waveforms shown Fig.7 (b), it is clear that the required output voltages are maintained under the proposed control scheme. Fig.7 (c) shows the voltage ripple of each output voltage corresponding to switching states which is discussed in theory. The control strategy is tested under disturbances in both load and input voltage, and the results are demonstrated in Fig.8 to Fig.10, respectively. In load variation test, two conditions have been considered. In one condition $R_2=50$ and R_1 is varied from 50 to 25Ω and back [Fig.8 (a) and (b)] and the other one $R_1=50$ and R_2 is varied from 50 to 25Ω and back [Fig.9 (a), (b)]. To show the effect of discontinuous modification of inductor reference current on dynamic response, two different times for modification, five and ten hysteresis cycle period, have been considered in each load variation condition. The output voltages displays an undershoot (overshoot) for the load current increase (decrease), but they quickly settle around their references value. As demonstrated in Fig.8 and Fig.9, modification of reference current each five cycles leads to superior dynamic response. Also, the switching options to control V_1 and V_2 , controlling of V_1 surpasses than the other output, so that it has less undershoot and overshoot compared with V_2 . While the converter is working with a load of $R_1=R_2=50 \Omega$ (CCM operation), a change in the input voltage from the $15-10 V$ and back is applied. The change in the input voltage and the corresponding output-voltage waveforms are depicted in Fig.10. It is observed that the total output voltage shows small undershoot (overshoot) for the input voltage increase (decrease) and settles down after a short time. However, the mid point voltage remains constant, and the transients in voltage are sufficiently diminished.

Conclusion

In this paper a simple and cost effective control strategy has been proposed to control the mid point voltage of MOB converter and also boost the low input voltage. Double-output MOB converter and discrete voltage control with inner hysteresis current control loop has been implemented by laboratory prototype. Simulation and experimental results verify the success of control strategy and performance of the proposed converters. Proposed control algorithm could easily be extended to offer multiple outputs by adding extra mid point voltage control block.

References

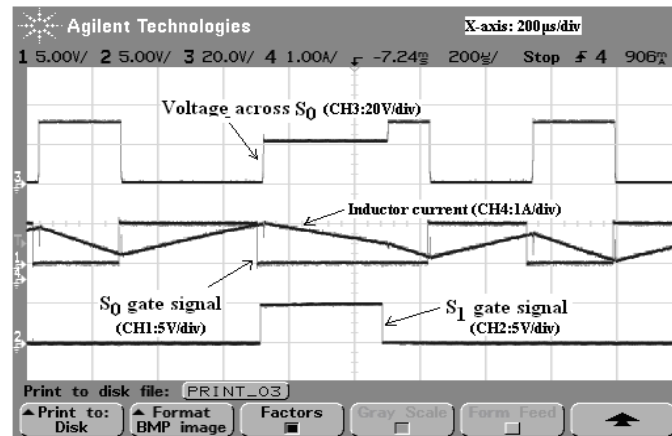
- [1] X.Yunxiang and G.Jiuchao, "Study on the voltage stability of multi-output Converters," IEEE IPEMC'2004, pp. 482-486, Vol. 2, August 2004.
- [2] A. Nami, F. Zare, G. Ledwich, A. Ghosh, and F. Blaabjerg, "A new configuration for multilevel converters with diode clamped topology," in IEEE IPEC'07., 2007, pp. 661-665.
- [3] R. Mammano, "Switching power supply topology voltage mode vs. current mode," Texas Instruments Incorporated 1999.
- [4] T. Siew-Chong, Y. M. Lai, and C. K. Tse, "Implementation of pulse-width-modulation based sliding mode controller for boost converters," IEEE Power Electronics Letters, , vol. 3, pp. 130-135, 2005.
- [5] R. Naim, G. Weiss, and S. Ben-Yaakov, " H_{∞} control applied to boost power converters," IEEE Transactions on Power Electronics., vol. 12, pp. 677-683, 1997.

[6] T. Siew-Chong, Y. M. Lai, C. K. Tse, L. Martinez-Salamero, and W. Chi-Kin, "A fast-response sliding-mode controller for boost-type converters with a wide range of operating conditions," IEEE Transactions on Industrial Electronics, vol. 54, pp. 3276-3286, 2007.

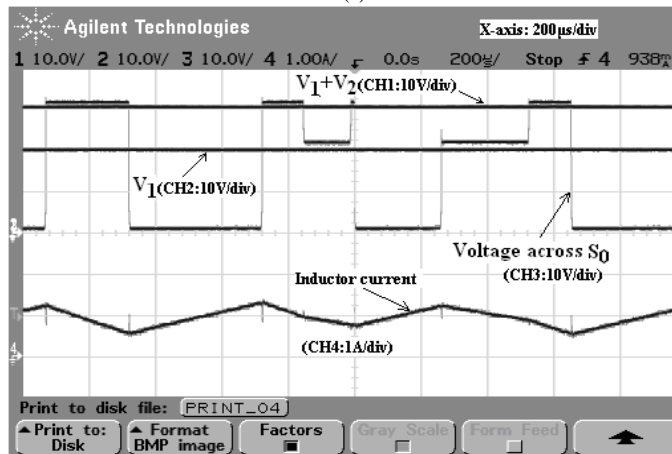
[7] J. Alvarez-Ramirez, I. Cervantes, G. Espinosa-Perez, P. Maya, and A. Morales, "A stable design of PI control for DC-DC converters with an RHS zero," IEEE Transactions on Circuits and Systems : Fundamental Theory and Applications, vol. 48, pp. 103-106, 2001.

[8] S. Chattopadhyay and S. Das, "A digital current-mode control technique for DC-DC Converters," IEEE Transactions on Power Electronics, , vol. 21, pp. 1718-1726, 2006.

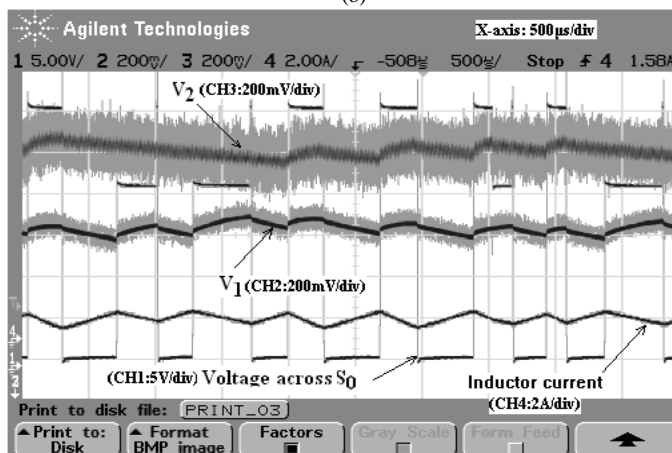
[9] H. Peng and D. Maksimovic, "Digital current-mode controller for DC-DC converters," in Twentieth Annual IEEE Applied Power Electronics Conference and Exposition, 2005. APEC 2005. , 2005, pp. 899-905 Vol. 2.



(a)

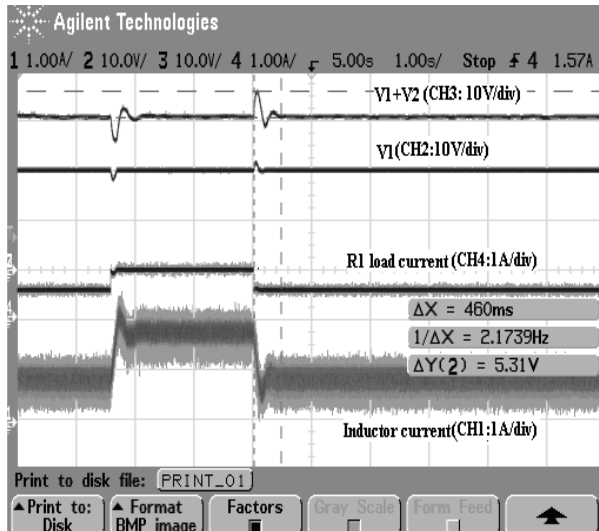


(b)

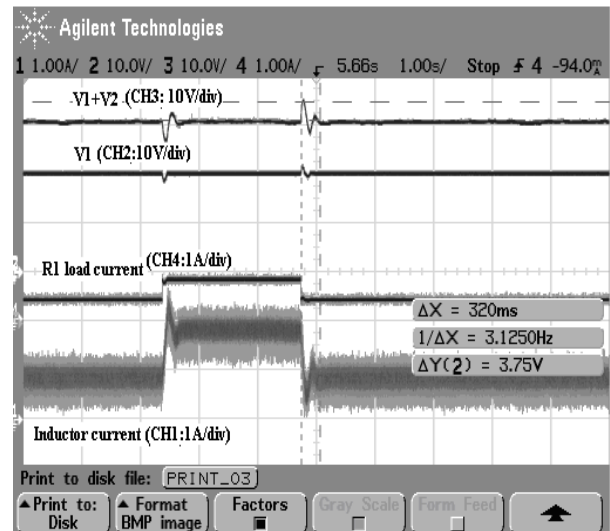


(c)

Fig.7: (a) Steady-state inductor current and switching pulses for the CCM operation ($R_l = 50 \Omega$ and $R_2=50 \Omega$). (b) Output voltages corresponding to (a). (c) Output voltages ripple regarding to switching states

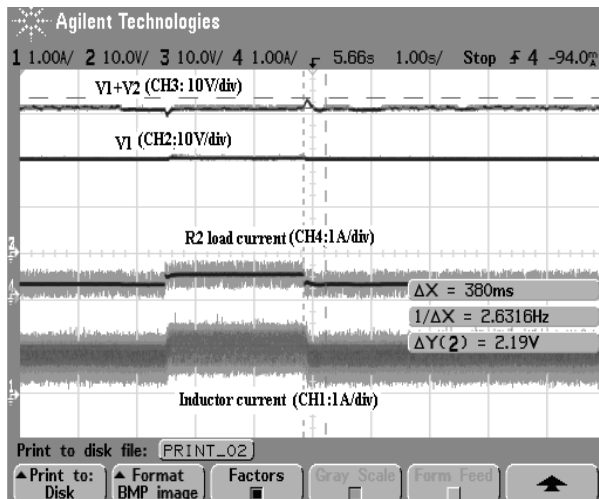


(a)

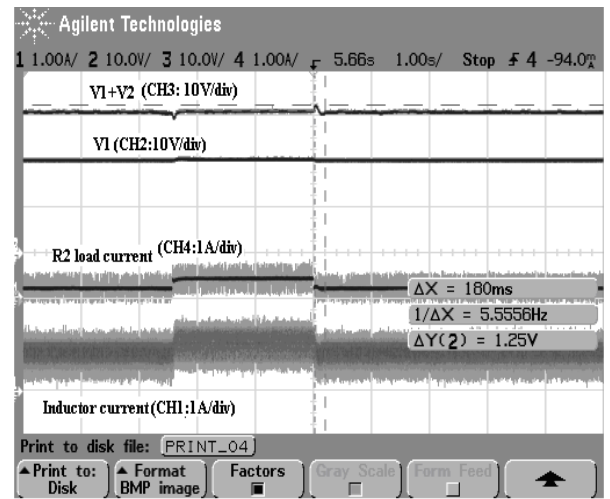


(b)

Fig. 8: Waveforms during transient condition when R_1 is changed form 50Ω to 25Ω and $R_2=50 \Omega$. (a) current modification after 10 hysteresis cycles (b) current modification after 5 hysteresis



(a)



(b)

Fig. 9: Waveforms during transient condition when R_2 is changed form 50Ω to 25Ω and $R_1=50 \Omega$. (a) current modification after 10 hysteresis cycles (b) current modification after 5 hysteresis

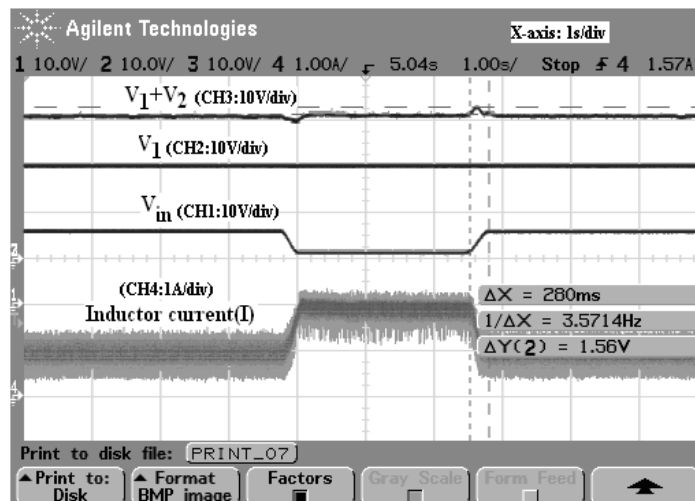


Fig. 10: Output voltage during input voltage disturbance from $15V$ to $10V$ back to $10V$ ($R_1=R_2=50 \Omega$)